JOURNAL OF CHEMICAL INFORMATION AND MODELING

Article

pubs.acs.org/jcim

Computational Comparison of Imidazoline Association with the I2 Binding Site in Human Monoamine Oxidases

Livia Basile,[†] Matteo Pappalardo,[‡] Salvatore Guccione,*[,†,§] Danilo Milardi,[∥] and Rona R. Ramsay*[,⊥]

[†]Etnalead s.r.l., c/o EtnaBuilding, Scuola Superiore di Catania, Università degli Studi di Catania, via S. Nullo 5/i, I-95123 Catania, Italy

[‡]Dipartimento di Scienze Chimiche, Università degli Studi di Catania, Viale A.Doria 6 Ed.3, Città Universitaria, I- 95125 Catania, Italy

[§]Dipartimento di Scienze del Farmaco, Università degli Studi di Catania, Viale A.Doria 6 Ed. 2, Città Universitaria, I-95125 Catania, Italy

[∥]IBB-CNR, Istituto di Biostrutture e Bioimmagini, UOS di Catania c/o Dipartimento di Scienze Chimiche, Università degli Studi di Catania, Viale A.Doria 6 Ed.3, Città Universitaria, I- 95125 Catania, Italy

[⊥]Biomedical Sciences Research Complex, University of St. Andrews, North Haugh, St. Andrews KY16 8QP, U.K.

ABSTRACT: Imidazoline ligands in I2-type binding sites in the brain alter monoamine turnover and release. One example of an I2 binding site characterized by binding studies, kinetics, and crystal structure has been described in monoamine oxidase B (MAO B). MAO A also binds imidazolines but has a different active site structure. Docking and molecular dynamics were used to explore how 2-(2-benzofuranyl)-2-imidazoline hydrochloride (2-BFI) binds to MAO A and to explain why tranylcypromine increases tight binding to MAO B. The energy for 2-BFI binding to MAO A was comparable to that for tranylcypromine-modified MAO B, but the location of 2-BFI in the MAO A could be anywhere in the monopartite substrate cavity. Binding to the tranylcypromine-modified MAO B was with high affinity and in the entrance cavity as in the crystal structure, but the energies of interaction with the native MAO B were less favorable. Molecular dynamics revealed that the entrance cavity of MAO B after tranylcypromine modification is both smaller and less flexible. This change in the presence of tranylcypromine may be responsible for the greater affinity of tranylcypromine-modified MAO B for imidazoline ligands.

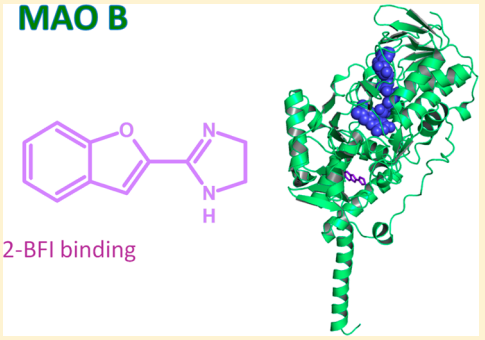

1. INTRODUCTION

Ligands for the imidazoline type 2 (I2) binding sites in the brain alter monoamine turnover and release. Endogenous ligands for the I2 binding sites include harmane and agmatine. Ligands such as idazoxan (nonselective) and 2-(2-benzofuranyl)-2-imidazoline hydrochloride (2-BFI) have high affinity (nanomolar) for these sites. The pharmacology of I2 binding sites has been established and some structure−activity studies reported.[1] A recent imaging study revealed a distribution in the brain consistent with known levels measured functionally.[2] However, the identity of the proteins that provide these I2 binding sites remains controversial. One protein known to bind imidazoline ligands is monoamine oxidase (MAO).

High-affinity I2 binding sites[3] were convincingly localized to MAO in 1995 when expression of human MAO A and MAO B in yeast resulted in a gain of previously nonexistent I2 ligand binding with nanomolar affinity.[4] Some MAO substrates and inhibitors bind to I2 binding sites, for example, harmane, a β-carboline formed from tryptamine, which has nanomolar affinity both for I2 binding sites and for MAO A.[4,5] Imidazolines also inhibit both MAO A and MAO B but with K_i values in the micromolar range.[4,6−11] Interestingly, the irreversible MAO inhibitor, tranylcypromine (TCP), was found to increase the binding of 2-BFI in rat and human brains. In contrast, inactivation of either rat MAO B or human MAO A with TCP did not increase the binding of 2-BFI.[12−14]

Kinetic studies have been used to explore whether the specific I2 ligand, 2-BFI, binds in the active site of MAO. In purified MAO A, the kinetic studies indicated only one type of binding. I2 ligands inhibited the activity of MAO A competitively, and spectral changes suggested that the binding site was close to the MAO A FAD cofactor.[11] However, it was reported that the kinetics for the inhibition of MAO B indicated noncompetitive inhibition, suggesting a binding site separate from the substrate binding site.[8] A subsequent binding and kinetics study using purified MAO B established that 2-(2-benzofuranyl)-2-imidazoline hydrochloride (2-BFI) binds both to the free enzyme and to the enzyme−substrate complex indicating that the high affinity 2-BFI binding is not in the part of the catalytic cavity that binds the substrate.[15]

The crystal structure of a MAO B-tranylcypromine (TCP)-2-BFI complex found 2-BFI bound in the entrance cavity of MAO B.[14,15] In native MAO B, about 10% of the total MAO B

Received: April 9, 2013
Published: March 6, 2014

binds 2-BFI at high affinity,[15] but inactivation of MAO B by TCP increases the high affinity binding to 100%. Both the native MAO B and the MAO B-TCP adduct forms with 2-BFI bound in the entrance site have been crystallized.[14] The structure of the MAO B-TCP-2-BFI complex revealed that the orientation of the gating residues between the entrance cavity and the catalytic cavity was important for binding. The complex with nanomolar affinity for 2-BFI had the Ile199 gate in the closed position and a different orientation of Gln206 from other MAO B-inhibitor complexes.[14] Although no other classic catalytic site inhibitor enhanced the high affinity binding, 2-BFI was also found in the entrance cavity in the crystal structure of rasagiline-inactivated MAO B. Even the mutation of the Ile199 residue to alanine did not change the location of 2-BFI in the crystal structure. The residues, Ile199, Ile316, Pro102, and Tyr326 form the binding site for 2-BFI in both the ternary MAO B-TCP-2-BFI complex and the binary MAO B-2-BFI complex, with hydrogen bonds between the furan ring of 2-BFI and the latter two residues. The crystal structures[14] clearly illustrate that the 2-BFI binding site at the gate between the entrance and catalytic cavities is present in all forms of MAO B, although high affinity binding is detected only in a small proportion of human MAO B molecules unless it has been inactivated by TCP to form the hMAO B-TCP complex.[15]

As found for rat MAO B, 2-BFI binding to MAO A is not enhanced by TCP,[13] but 2-BFI inhibits both membrane-bound and purified MAO A at micromolar concentrations. Although binding deep in the active site close to the flavin could explain the appearance of some I2 binding as detected when MAO A is expressed in yeast, it does not account for the nanomolar affinity reported for idazoxan in these experiments.[4] The active site of MAO A is monopartite, lacking the constriction or gate seen in MAO B as a result of the juxtaposition of Tyr326 and Ile199, but an overlay of MAO A and MAO B shows similar structure for the two enzymes around the 2-BFI binding site (Figure 1).[14,16,17] Of the four residues important in binding 2-BFI in the entrance cavity of MAO B, only one isoleucine is conserved in MAO A (Ile325). The gating residue Ile199 is conservatively substituted by Phe208, but the two residues in MAO B involved in hydrogen bonds to 2-BFI are replaced by Ala111 and Ile335. Thus, reduced affinity in MAO A is predictable, but the existence of a 2-BFI binding site equivalent to that found in MAO B remains a possibility as shown in Figure 1.

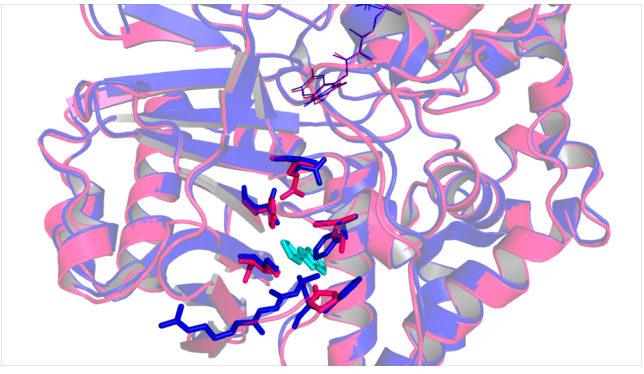

Figure 1. Comparison of the MAO A (PDB ID: 2Z5X,[17] blue) active site cavity with that of MAO B-TCP-2-BFI (PDB ID: 2XCG,[14] pink). The FAD cofactors are shown in line form. The residues in contact with 2-BFI (cyan) are displayed in stick format: Pro102, Ile199, Gln206, Ile316, and Tyr326 in MAO B (blue) with the equivalent residues Ala111, Phe208, Gln215, Ile325, and Ile335 in MAO A (pink). Residues 109−112 of the loop at the entrance to the active site cavity in MAO A are shown in blue stick format.

The purpose of this computational analysis of 2-BFI binding in oxidized, reduced, and TCP-inactivated MAO A and MAO B was 2-fold: to investigate why TCP increases the fraction of MAO B molecules that bind 2-BFI with nanomolar affinity; and to explore the possibility of a high affinity I_2 binding sites in MAO A or MAO B comparable to that in TCP-inactivated MAO B that could explain the binding measured in tissues.

2. MATERIALS AND METHODS

Molecular dynamics simulations and docking studies were carried out using an Intel Core i7 processor, RAM 16 GB, operating under Linux/Ubuntu 10.04. MAO A (PDB code: 2Z5X[17]) and MAO B (PDB code: 2XCG[14]) crystal structures were used. The TCP and 2-BFI structures were built and optimized using the software SYBYL-X 1.3 (http://www.tripos.com).

2.1. Molecular Dynamics (MD). The TCP and 2-BFI parameters were determined by the ParamChem tool available at the http://www.charmm-gui.org Web site. A total of eight systems were built. Starting points for the minimization and equilibration protocol and for the MD trajectories were in accordance with literature data with the cofactor covalently bound to Cys406 in MAO A and to Cys397 in MAO B.[18] The ring-opened form of TCP was covalently bound to the C(4a) position on the flavin by the benzyl carbon.[14,19] The system was solvated with pre-equilibrated water molecules in the three-dimensional space (box of water) of 84.32 × 187.67 × 97.66 Å edges. The counterions (Na^+ and Cl^-) were placed in the proximity of the regions of the protein surface to mimic an ionic strength of 0.15 mM.

MD simulations were carried out using NAMD2 software, version 2.9.[20] The forcefield adopted was CHARMM27 where all atoms are explicitly represented and water is characterized by the TIP3P model with 1 as the dielectric constant (ε).[21] All systems were energy-minimized (conjugate gradient) and gradually heated up to 300 K with a 2-fs time step and equilibrated with a 300 K thermal bath for 400 ps with the velocities being reassigned in the system every 2 ps to achieve complete stability.[22] Production runs were performed at 300 K. The SHAKE algorithm with a tolerance of 1×10^{-8} Å was used to fix the length of the covalent hydrogen bonds.[23] Non-covalent interactions were calculated at each step. To avoid edge effects and treat long-range electrostatic interactions, periodic boundary conditions and the particle-mesh-Ewald algorithm with a grid size of 84.32 × 187.67 × 97.66 Å,[24] respectively, were applied to all of the simulations steps. Nonbonded short-range interactions were treated by a cutoff value of 10 Å. One hundred nanoseconds of MD simulation for all systems were carried out. Only two systems (MAO A oxidized ± TCP) were examined after 20 ns of MD since there were no evident changes in terms of docking scores after 100 ns of MD. Analyses of the trajectories were performed using the VMD 1.91 software.[25] The average structures as obtained from the last xyz atomic coordinates (50 ps for each MD simulation) were used in docking analysis.

2.2. Docking Analysis. Side-chain flexible ligand-protein docking was carried out by the molecular docking algorithm MolDock Optimizer[26] and the scoring function MolDock [GRID] as implemented in Molegro Virtual Docker software, version 6. Only torsion angles in the side chains were modified

dx.doi.org/10.1021/ci400346k | J. Chem. Inf. Model. 2014, 54, 1200−1207

during the minimization; all other properties, including bond lengths and backbone atom positions, were held fixed, and a new receptor conformation was generated for each pose after side chain flexible docking calculation. Protein residues Ala111, Phe208, Ile325, and Ile335 in hMAO A were set as flexible; these residues correspond to Pro102, Ile199, Ile316, and Tyr326 in hMAO B, which belong to the architecture of the 2-BFI binding site as reported in ref 14. Potentials were softened to a value of 1.5 and 0.5 for tolerance and strength, respectively. The 70 runs for each molecule were carried out with a population size of 50, maximum iteration of 1500, scaling factor of 0.50, crossover rate of 0.90, and a variation-based termination scheme. Poses within a root-mean square deviation of 1.5 Å were clustered together by means of the "Tabu pose" clustering algorithm.

3. RESULTS

3.1. Comparison of Human MAO Structures without and with 2-BFI. The similarity of the MAO A structure at the entrance to the active site to that of MAO B is apparent in Figure 1, with the key residues for 2-BFI binding conservatively substituted as indicated in the legend. Only Phe208 in the unliganded MAO A structure is badly placed for 2-BFI binding.

For MAO B, the highly informative crystallography work[14] has compared the binding site for 2-BFI in three ligand states of MAO B, namely, MAO B with both TCP and 2-BFI bound (PDB ID: 2XCG) shown in green in Figure 2; MAO B with only TCP in orange (PDB ID: 2XFU); and MAO B with only 2-BFI in cyan (PDB ID: 2XFN). The 2-BFI binding sites of these three structures are overlaid in Figure 2. As noted by McDonald et al.,[15] the structure where the MAO B flavin is modified with TCP and 2-BFI is bound differs from the other structures, in that Pro102 and the cavity-shaping loop of which it is part are slightly displaced. This difference suggests that adjustment of the residues could be important for high affinity.

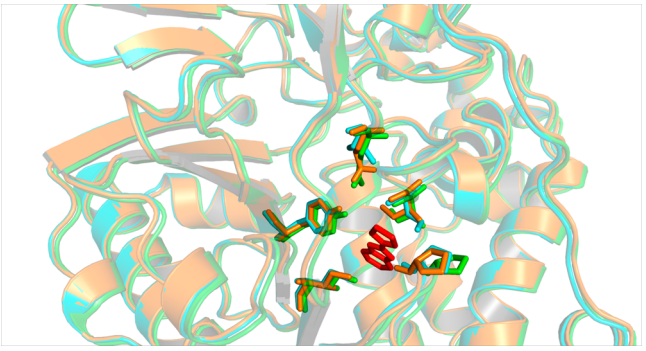

Figure 2. Overlay of the three structures of MAO B from Bonivento et al.[14] Orange, MAO B reduced and modified by TCP (PDB ID: 2XFU); cyan, MAO B with 2-BFI (PDB ID: 2XFN); green, MAO B reduced and modified by TCP with 2-BFI (PDB ID: 2XCG).

3.2. Comparison of the Dynamic Binding of 2-BFI to MAO A and B. MD simulations were performed for both enzymes, MAO A and MAO B, with the FAD cofactor (oxidized or reduced) covalently bonded to Cys406 and Cys397, respectively, in the presence or absence of TCP. Specifically, the systems considered in the analysis were as follows.

MAO A: MAO A oxidized, MAO A-FAD in the oxidized state with no ligands bound; MAO A reduced, MAO A-FADH in the reduced state with no ligands bound; TCP MAO A oxidized, MAO A-FAD in the oxidized state with TCP reversibly docked; and TCP-MAO A reduced, MAO A-FADH in reduced state and modified at C4a by TCP.

MAO B: MAO B oxidized, MAO B with FAD in the oxidized state and no ligands bound; MAO B reduced, MAO B-FADH in the reduced state and no ligands bound; TCP MAO B oxidized, MAO B-FAD in the oxidized state with TCP reversibly docked; and TCP-MAO B reduced, MAO B-FADH in the reduced state and modified at C4a by TCP.

For all these systems, snapshots (average structures) obtained by the MD protocol described in Materials and Methods were used for docking analysis. The ligand, 2-BFI, was docked in the whole active site or in the entrance cavity of the proteins. Protein residues Ala111, Phe208, Ile325, and Ile335 in hMAO A were set as flexible; these residues correspond to the MAO B residues, Pro102, Ile199, Ile316, and Tyr326, belonging to architecture of the entrance cavity.[14] The interaction energies between 2-BFI and the protein, obtained by docking calculations, are shown in Table 1.

Table 1. Interaction Energies (kcal/mol) of 2-BFI with MAO A and MAO B

	interaction[a]	protein[b]	MolDockScore[c]
MAO A oxidized	−93.85	−93.34	−104.59
TCP MAO A oxidized	−90.95	−86.25	−101.56
MAO-A reduced	−89.50	−89.50	−88.98
TCP-MAO A reduced	−81.35	−81.35	−80.83
MAO B oxidized	−59.75	−59.75	−59.33
TCP MAO B oxidized	−87.95	−87.95	−99.20
MAO-B reduced	−60.04	−60.04	−59.62
TCP-MAO B reduced	−91.88	−91.88	−91.33

[a]Total energy of interaction between the ligand and the target molecule. [b]Energy of interaction between the ligand and the protein. [c]Evaluated energy after docking.

Table 1 shows that the binding of 2-BFI to MAO B changes when TCP is present. Binding is strongly increased both when TCP is reversibly docked to the oxidized form of the enzyme and after the suicide reaction has generated the reduced flavin covalently modified by TCP. Thus, for MAO B, both reversible binding of TCP and TCP modification of MAO B (accompanied by reduction of the flavin) favor the binding of 2-BFI. Looking at the space available for 2-BFI binding, analysis of the average structures of MAO B with and without TCP shows that, as expected, the substrate cavity of MAO B in the presence of TCP is smaller than in its absence. The volumes are for the oxidized enzyme, 1096 Å^3 in MAO B oxidized and 215 Å^3 in MAO B oxidized with TCP reversibly bound; and for the reduced enzyme, 460 Å^3 in MAO B reduced and 335 Å^3 in TCP-MAO B reduced.

The favorable and unfavorable interactions of 2-BFI with the amino acid residues in the entrance cavity of MAO B binding site after the MD equilibration of the protein structures and subsequent docking are shown in Table 2. At first glance, the presence of TCP decreases the number of unfavorable energy interactions of the MAO B-cofactor complex in both redox states. Looking at the details of the residues interacting with 2-BFI, TCP decreases the steric hindrance with Tyr 326 seen in MAO B oxidized and reduced, stabilizing the protein−ligand interaction (Table 2 and Figure 3). Note in particular that the

dx.doi.org/10.1021/ci400346k | J. Chem. Inf. Model. 2014, 54, 1200−1207

Table 2. Favorable and Unfavorable Interaction Energies (kcal/mol) for Entrance Cavity Residues Contacting 2-BFI in MAO A and MAO B[a]

MAO A				MAO B			
favorable		unfavorable		favorable		unfavorable	
residue	energy	residue	energy	residue	energy	residue	energy
			Oxidized				
Ile 180	−11.60	Phe 208	20.51	Pro 102	−10.63	Gly 101	1.25
Asn 181	−9.11	Ile 335	4.24	Ser 200	−9.52	Ile 199	9.36
Gln 215	−9.53			Thr 201	−5.75	Tyr 326	10.59
			Oxidized + TCP				
Phe 177	−12.33			Pro 102	−9.91	Leu 88	0.97
Ile 180	−9.92			Pro 103	−7.75		
Ile 207	−6.32			Ile 199	−17.7		
Phe 208	−12.90			Tyr 326	−14.77		
			Reduced				
Phe 208	−8.17			Phe 99	−8	Pro 104	14.53
Ser 209	−8.51			Phe 103	−6.59	Ile 199	61.08
Val 210	−15.07					Ile 199	19.85
Gln 215	−18.11					Tyr 326	29.96
Ile 335	−5.45						
Leu 337	−6.81						
			Reduced TCP-Adduct				
Phe 108	−5.15	Phe 208	2.4	Pro 102	−7.21		
Ala 111	−6.40			Phe 103	−13.12		
Pro 113	−7.14			Leu 167	−5.94		
Leu 176	−7.14			Phe 168	−8.17		
Phe 177	−12.14			Ser 200	−5.64		
Ile 180	−6.90			Ile 316	−7.06		
Ser 209	−6.42			Tyr 326	−5.89		
Ile 325	−7.54						

[a]Values better than −5 are reported for the favorable interactions.

gating residue Tyr326 makes a highly unfavorable contact with 2-BFI in the unliganded MAO B, but when TCP is bound, this residue contributes favorably to the binding. Ile199 in MAO B also gives highly unfavorable interactions in free enzyme that disappear when TCP is bound.

As described above, TCP binding reverses the interaction with Tyr326 from unfavorable to favorable, and the reduction of the flavin changes the interactions of 2-BFI with the entrance cavity residues (Figure 3). Snapshots of 2-BFI in the entrance cavity revealed that 2-BFI in three of the forms, the MAO B oxidized, reduced, and TCP MAO B oxidized, makes one H bond with Tyr326, although unfavorable steric clashes predominate (Table 2). Analysis of the reduced form of MAO B showed that 2-BFI forms a H bond (to Trp119) only in the presence of the TCP adduct. The energy analysis (Table 1) suggests that the conformation held when TCP is present contributes to the high affinity binding of 2-BFI. It should be noted that the rasagiline-2-BFI-MAO-B complex 2XFQ[14] is in the reduced form and has an occupied catalytic cavity but that the gate is open, and no high affinity binding of 2-BFI was found. Prediction of the *in vivo* induction of this conformation to bind 2-BFI may be difficult and may require each candidate to be examined experimentally and by crystal structure.

Turning to MAO A, it is obvious from Table 1 that TCP does not enhance the binding of 2-BFI to the active site of MAO A. The energy values for MAO A show that there is no detectable energy difference between 2-BFI interaction to the TCP-liganded and ligand-free forms of the MAO A active site, indicating no positive effect by TCP on the binding mode.

The energy values (Table 1) indicate binding of 2-BFI to all MAO A receptor forms. In MAO A oxidized, there is one H bond with 2-BFI (Phe 208), as opposed to TCP MAO A oxidized that does not form a H bond with ligand. Yet, in reduced MAO A there were no H bonds, but in reduced TCP-MAO A, Phe 208 forms a H bond with 2-BFI. For other interactions of note, Table 2 indicates an unfavorable clash with Phe208 in MAO A oxidized as expected from inspection of the crystal structure overlay in Figure 1. This clash disappears in the other forms. The unfavorable interaction with Ile335 (equivalent to Tyr326 in MAO B) disappears when TCP is bound (Table 2), but it makes very little difference to the overall energy of binding (Table 1). The overall energy values clearly indicate that TCP does not affect the interaction of 2-BFI with MAO A, in agreement with reported experimental observations.

However, changes in interactions are seen between oxidized and reduced forms of MAO A; reduction in MAO A makes 2-BFI binding less favorable (Table 1). Clearly, the redox state of the flavin influences the conformation of the active site changing the ligand interactions. In contrast to MAO B, reduction of MAO A induces an enlargement of the receptor cavity. The space available for 2-BFI binding in oxidized MAO A is 192 Å^3 but increases to 1270 Å^3 in MAO A reduced, while for the TCP-liganded MAO A, the space increases slightly from 269 Å^3 in the oxidized form to 300 Å^3 in TCP-MAO A reduced, enlargements that will decrease close contact with the ligand.

When the whole of the MAO A cavity was examined, 2-BFI contacts were found in all parts of the cavity (data not listed).

dx.doi.org/10.1021/ci400346k | J. Chem. Inf. Model. 2014, 54, 1200−1207

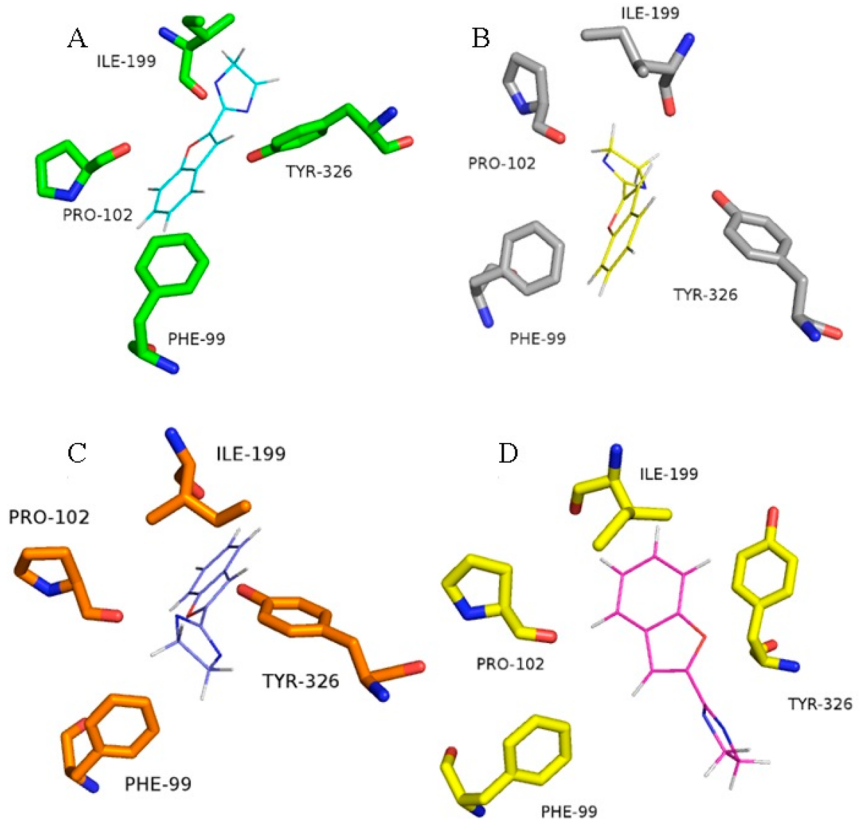

Figure 3. Best poses of 2-BFI in the entrance cavity of MAO B: (A) MAO B oxidized; (B) TCP MAO B oxidized; (C) MAO B reduced; and (D) TCP-MAO B reduced.

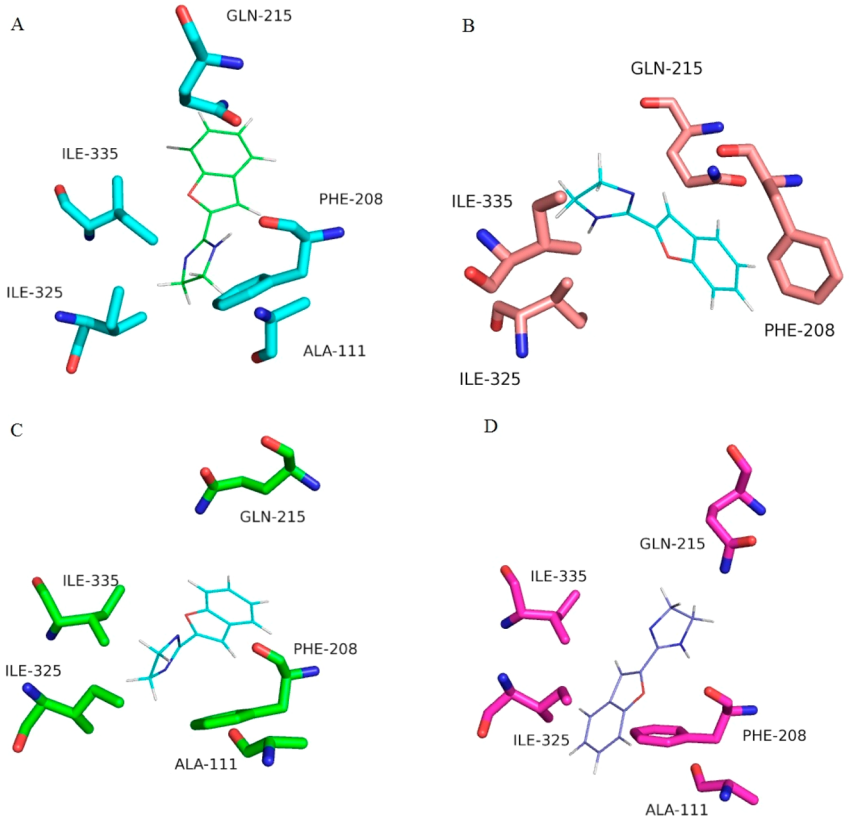

Figure 4. Best poses of 2-BFI docked into MAO A: (A) MAO A oxidized; (B) MAO A oxidized with TCP; (C) MAO A reduced; and (D) TCP-MAO A reduced.

dx.doi.org/10.1021/ci400346k | J. Chem. Inf. Model. 2014, 54, 1200−1207

The contacts are different from MAO B in terms of the atoms involved, distance, and strength, indicating a different mode of interaction in MAO A. Figure 4 illustrates typical poses for 2-BFI in MAO A. Without another ligand present, 2-BFI sits well into the monoapartite cavity of MAO A (Figure 4A and C) as indicated by favorable contacts with Gln215 and Asn181 (Table 2). The presence of TCP, either reversibly bound or after adduct formation, shifts the 2-BFI to the location equivalent to the entrance cavity of MAO B (Figure 4B and D), although residues near Phe208 orient the 2-BFI differently in the oxidized, reversibly liganded, or reduced TCP-modified forms.

3.3. Molecular Dynamics of the Loop Important for Substrate Binding. Further MD analyses were carried out to study the flexibility of the MAO A loop 109−112 next to the entrance (109−112 in MAO A;[17] 100−103 in MAO B[19]), which was suggested to be critical for opening the entrance for substrate or inhibitors. The loop in MAO B includes Pro102 that is the key to binding 2-BFI (Figure 3). The RMSDs of the loop 109−112 are reported in Figure 5 for MAO A without and

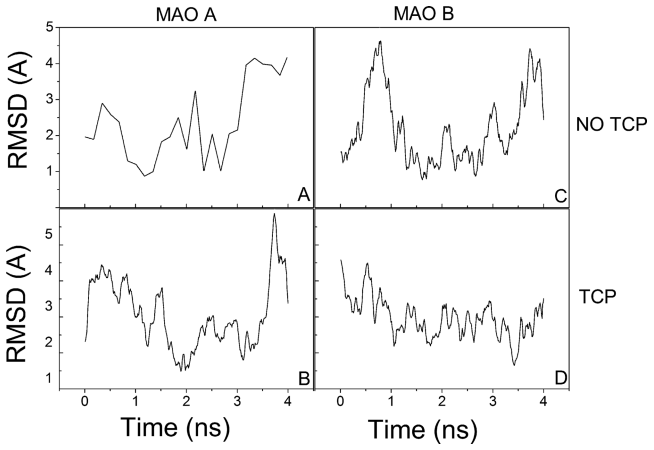

Figure 5. Flexibility in MAO A and B indicated by the RMSD of the entrance loop after 20 ns of MD. The left panels report the RMSD of the loop 109−112 from the minimized structure of MAO A; the right panels present the RMSD of the equivalent loop 100−103 MAO B. The top panels are without ligand and the bottom panels with TCP covalently bound. A, MAO A oxidized; B, MAO B oxidized; C, TCP-MAO A reduced; and D, TCP-MAO B reduced.

with TCP (left panels), and the same for the 100−103 loop in the MAO B oxidized form without TCP and with TCP covalently bound (right panels). From the RMSD profiles that indicate the amount of movement of the loop from its mean position, it appears that covalent bonding of TCP to MAO B makes the protein less flexible. The RMSD values go over 4 Å in the absence of TCP. Thus, the presence of TCP in the active site slows the motion of the cavity shaping loop, a feature that could result in the greater affinity of the TCP-MAO B adduct for 2-BFI.

4. DISCUSSION

I2 binding sites have proven difficult to identify and may not exist as one unique protein.[27,28] I2 binding to MAO B is the best characterized.[4] Previous work on MAO A provided evidence that I2 ligands bound near the flavin, acting as competitive inhibitors of MAO A in the active site.[11] This conclusion was based (1) on the ability of agmatine to act as a substrate reducing MAO A, (2) on spectral changes at 500 nm on binding, and (3) on the ability of guanabenz to stabilize the semiquinone species, all indicating proximity to the flavin.[11] Docking studies at that time could only analyze placement near the flavin after a tether was introduced to keep the small molecule near the covalently bound flavin. Here, the binding of the I2 ligand, 2-BFI, has been analyzed by MD on the cavities of both MAO A and MAO B without and with TCP, and in both oxidized and reduced states. The evidence from docking and molecular dynamics shows that 2-BFI can bind in the active site of MAO A. More importantly, the results on the MAO B entrance cavity provide insight into why TCP improves the binding of 2-BFI to MAO B.

4.1. 2-BFI Binding in the Entrance Cavity of MAO B Varies with Redox State and TCP Modification. In light of the structures for MAO B and for MAO B-TCP with 2-BFI bound,[14] the binding of I2 ligands at the entrance cavities of MAO A and MAO B has been examined by MD. The 2-BFI binding in unliganded enzyme is energetically less favorable than in the TCP-modified MAO B but may be sufficient to explain the binding observed in native MAO B (<10%). The alternate explanation is that only a small part of the population of unliganded MAO B molecules are in a suitable conformation for 2-BFI binding during normal molecular motion in unliganded, unmodified enzymes. When MAO B is modified by TCP, the smaller entrance cavity and the lower mobility of the entrance loop may be key in creating the high affinity binding site in the modified enzyme, converting the whole population into the appropriate conformation. The lower mobility of the loop at the entrance to the substrate cavity may also hinder dissociation resulting in a longer residence time that equates with higher affinity.

It is notable that the energy for the binding of 2-BFI to the reduced form of MAO B is quite similar to the oxidized form, but in the reduced MAO B, the unfavorable interactions are more and higher. A lower affinity between 2-BFI and the reduced MAO B was found experimentally by determining the K_i for the oxidized or reduced MAO B in alternative kinetic pathways. The K_i for inhibition via the oxidized pathway was 7.9 ± 1.0 μM but via the reduced pathway was 326 ± 35 μM.[15]

4.2. Does 2-BFI Bind to MAO A? In MAO A with its monopartite cavity, the many interactions found show that the ligand can take up a variety of poses throughout the whole active site, many of them closer to the flavin than seen in MAO B. It seems probable that the open monopartite cavity of MAO A allows free diffusion toward the flavin unlike the gated cavity in MAO B, where a closed gate seems to facilitate the high affinity binding.[14,15] That TCP does not have the same positive effect on 2-BFI binding in MAO A may result from the lack of this gate, yet the poses found in MAO A in the presence of TCP do suggest that steric hindrance keeps 2-BFI in the outer part of the cavity at least in the oxidized form. The increase in the size of the cavity upon reduction or TCP binding in MAO A is a major factor likely to exclude any close contact with the ligand.

4.3. Impact of Flexibility in MAO B. Docking with flexibility in both the ligand and the surrounding active site residues yields energy results consistent with the reduced MAO B-TCP adduct forming a high affinity binding site for 2-BFI with the Ile199-Tyr326 gate closed, as observed in the crystal structure. The differences in space available for binding suggest considerable flexibility in the active site, confirmed by changes in conformation depending on redox state and ligand binding observed experimentally at least for MAO A.[29]

The present MD study shows that MAO A has an open cavity with no change in the flexibility of the entrance cavity loop on TCP binding, whereas for MAO B there is less flexibility in the TCP-modified MAO B than in the unliganded enzyme (Figure 5). A study using in depth atomistic molecular dynamic simulations of MAO B in the membrane found that access to the active site was influenced by the interaction with the membrane and in particular by the movement of two loops 85−110 and 155−165.[30] Although the data presented here cover only residues 100−103, this part of the cavity loop shows a distinct decrease in flexibility after reduction and modification of MAO B with TCP, leading to the hypothesis that the less mobile entrance cavity loop favors 2-BFI binding and perhaps also hinders dissociation.

5. CONCLUSIONS

With developing interest in the discovery of I2 ligands[30−32] for use as drugs, better understanding of the MAO B-associated I2 binding site would be useful. It is a major conceptual difficulty that TCP-modified MAO B, the only structurally characterized I2 binding site, is a very artificial state: very few patients for whom I2 ligands might be beneficial have been treated with TCP. Co-treatment with TCP hardly seems advisable, so the pharmacological questions remain, especially regarding why I2 binding sites increase with age and whether 2-phenylethylamine, an endogenous inactivator of MAO B, acts to increase I2 binding sites *in vivo*. 2-Phenylethylamine has been shown to mimic the effect of TCP and increase the high affinity binding of 2-BFI to MAO B.[15] The next step in medicinal chemistry is to investigate structure−activity correlations using molecular dynamics and enzymology so that clear links between these studies and the pharmacology of these elusive sites can be determined.

AUTHOR INFORMATION

Corresponding Authors

*(S.G.) Tel: +39 095 738-4020. Fax: +39 095 738-4208. E-mail: guccione@unict.it.

*(R.R.R.) Tel: +44 1334 463411. Fax: +44-1334-462595. E-mail: rrr@st-and.ac.uk.

Author Contributions

R.R.R. and S.G. conceived and designed the experiments. L.B., M.P., and D.M. performed the experiments. L.B., M.P., D.M., S.G., and R.R.R. analyzed the data. R.R.R. and S.G. wrote the paper.

Notes

The authors declare no competing financial interest.

ACKNOWLEDGMENTS

R.R.R. thanks the Carnegie Trust for a travel award and Chiara Platania for her initial docking experiments.

REFERENCES

(1) Dardonville, C.; Rozas, I. Imidazoline binding sites and their ligands: An overview of the different chemical structures. *Med. Res. Rev.* **2004**, *24*, 639−661.

(2) Kealey, S.; Turner, E. M.; Husbands, S. M.; Salinas, C. A.; Jakobsen, S.; Tyacke, R. J.; Nutt, D. J.; Parker, C. A.; Gee, A. D. Imaging imidazoline-I-2 binding sites in porcine brain using C-11-BU99008. *J. Nucl. Med.* **2013**, *54*, 139−144.

(3) Miralles, A.; Olmos, G.; Sastre, M.; Barturen, F.; Martin, I.; García-Sevilla, J. A. Discrimination and pharmacological characterization of I-2-imidazoline sites with H-3 idazoxan and alpha-2 adrenoceptors with H-3 Rx821002 (2-methoxy idazoxan) in the human and rat brains. *J. Pharmacol. Exp. Ther.* **1993**, *264*, 1187−1197.

(4) Tesson, F.; Limon-Boulez, I.; Urban, P.; Puype, M.; Vandekerckhove, J.; Coupry, I.; Pompon, D.; Parini, A. Localization of I-2-imidazoline binding-sites on monoamine oxidases. *J. Biol. Chem.* **1995**, *270*, 9856−9861.

(5) Musgrave, I. F.; Badoer, E. Harmane produces hypotension following microinjection into the RVLM: possible role of I-1-imidazoline receptors. *Br. J. Pharmacol.* **2000**, *129*, 1057−1059.

(6) Carpene, C.; Collon, P.; Remaury, A.; Cordi, A.; Hudson, A.; Nutt, D.; Lafontan, M. Inhibition of amine oxidase activity by derivatives that recognize imidazoline I-2 sites. *J. Pharmacol. Exp. Ther.* **1995**, *272*, 681−688.

(7) Gargalidis-Moudanos, C.; Pizzinat, N.; JavoyAgid, F.; Remaury, A.; Parini, A. I-2-imidazoline binding sites and monoamine oxidase activity in human postmortem brain from patients with Parkinson's disease. *Neurochem. Int.* **1997**, *30*, 31−36.

(8) Ozaita, A.; Olmos, G.; Boronat, M. A.; Lizcano, J. M.; Unzeta, M.; García-Sevilla, J. A. Inhibition of monoamine oxidase A and B activities by imidazol(ine)/guanidine drugs, nature of the interaction and distinction from I-2-imidazoline receptors in rat liver. *Br. J. Pharmacol.* **1997**, *121*, 901−912.

(9) Lalies, M. D.; Hibell, A.; Hudson, A. L.; Nutt, D. J. Inhibition of central monoamine oxidase by imidazoline(2) site-selective ligands. *Ann. N.Y. Acad. Sci.* **1999**, *881*, 114−117.

(10) Raasch, W.; Muhle, H.; Dominiak, P. Modulation of MAO activity by imidazoline and guanidine derivatives. *Ann. N.Y. Acad. Sci.* **1999**, *881*, 313−331.

(11) Jones, T. Z. E.; Giurato, L.; Guccione, S.; Ramsay, R. R. Interactions of imidazoline ligands with the active site of purified monoamine oxidase A. *FEBS J.* **2007**, *274*, 1567−1575.

(12) Wiest, S. A.; Steinberg, M. I. Binding of H-3 2-(2-benzofuranyl)-2-imidazoline (BFI) to human brain: Potentiation by tranylcypromine. *Life Sci.* **1997**, *60*, 605−615.

(13) Steinberg, M. I.; Wiest, S. A.; Pickard, R. T.; Chen, K.; Shih, J. C. Binding of the imidazoline ligand H-3−2-benzofuranyl-2- imidazoline (BFI) to human brain and platelets - Potentiation by tranylcypromine and role of MAO isoforms. *Ann. N.Y. Acad. Sci.* **1999**, *881*, 193−198.

(14) Bonivento, D.; Milczek, E. M.; McDonald, G. R.; Binda, C.; Holt, A.; Edmondson, D. E.; Mattevi, A. Potentiation of ligand binding through cooperative effects in monoamine oxidase B. *J. Biol. Chem.* **2010**, *285*, 36849−36856.

(15) McDonald, G. R.; Olivieri, A.; Ramsay, R. R.; Holt, A. On the formation and nature of the imidazoline I(2) binding site on human monoamine oxidase-B. *Pharmacol. Res.* **2010**, *62*, 475−488.

(16) De Colibus, L.; Li, M.; Binda, C.; Lustig, A.; Edmondson, D. E.; Mattevi, A. Three-dimensional structure of human monoamine oxidase A (MAO A): Relation to the structures of rat MAO A and human MAO B. *Proc. Natl. Acad. Sci. U.S.A.* **2005**, *102*, 12684−12689.

(17) Son, S. Y.; Ma, A.; Kondou, Y.; Yoshimura, M.; Yamashita, E.; Tsukihara, T. Structure of human monoamine oxidase A at 2.2-angstrom resolution: The control of opening the entry for substrates/inhibitors. *Proc. Natl. Acad. Sci. U.S.A.* **2008**, *105*, 5739−5744.

(18) Bach, A. W. J.; Lan, N. C.; Johnson, D. L.; Abell, C. W.; Bembenek, M. E.; Kwan, S. W.; Seeburg, P. H.; Shih, J. C. cDNA cloning of human-liver monoamine oxidase-A and oxidase-B - molecular basis of differences in enzymatic properties. *Proc. Natl. Acad. Sci. U.S.A.* **1988**, *85*, 4934−4938.

(19) Binda, C.; Li, M.; Hubalek, F.; Restelli, N.; Edmondson, D. E.; Mattevi, A. Insights into the mode of inhibition of human mitochondrial monoamine oxidase B from high-resolution crystal structures. *Proc. Natl. Acad. Sci. U.S.A.* **2003**, *100*, 9750−9755.

(20) Phillips, J. C.; Braun, R.; Wang, W.; Gumbart, J.; Tajkhorshid, E.; Villa, E.; Chipot, C.; Skeel, R. D.; Kale, L.; Schulten, K. Scalable molecular dynamics with NAMD. *J. Comput. Chem.* **2005**, *26*, 1781−1802.

(21) Jorgensen, W. L.; Chandrasekhar, J.; Madura, J. D.; Impey, R. W.; Klein, M. L. Comparison of simple potential functions for simulating liquid water. *J. Chem. Phys.* **1983**, *79*, 926−935.

(22) Berendsen, H. J. C.; Postma, J. P. M.; Vangunsteren, W. F.; Dinola, A.; Haak, J. R. Molecular-Dynamics with Coupling to an External Bath. *J. Chem. Phys.* **1984**, *81*, 3684−3690.
(23) Ryckaert, J. P.; Ciccotti, G.; Berendsen, H. J. C. Numerical-integration of cartesian equations of motion of a system with constraints - molecular-dynamics of N-alkanes. *J. Comput. Phys.* **1977**, *23*, 327−341.
(24) Essmann, U.; Perera, L.; Berkowitz, M. L.; Darden, T.; Lee, H.; Pedersen, L. G. A smooth particle mesh Ewald method. *J. Chem. Phys.* **1995**, *103*, 8577−8593.
(25) Humphrey, W.; Dalke, A.; Schulten, K. VMD: Visual molecular dynamics. *J. Mol. Graphics Modelling* **1996**, *14*, 33−38.
(26) Thomsen, R.; Christensen, M. H. MolDock: a new technique for high-accuracy molecular docking. *J. Med. Chem.* **2006**, *49*, 3315−3321.
(27) Kimura, A.; Tyacke, R. J.; Robinson, J. J.; Husbands, S. M.; Minchin, M. C. W.; Nutt, D. J.; Hudson, A. L. Identification of an imidazoline binding protein: Creatine kinase and an imidazoline-2 binding site. *Brain Res.* **2009**, *1279*, 21−28.
(28) Li, J.-X.; Zhang, Y. Imidazoline I-2 receptors: Target for new analgesics? *Eur. J. Pharmacol.* **2011**, *658*, 49−56.
(29) Hynson, R. M. G.; Kelly, S. M.; Price, N. C.; Ramsay, R. R. Conformational changes in monoamine oxidase A in response to ligand binding or reduction. *Biochim. Biophys. Acta, Gen. Subj.* **2004**, *1672*, 60−66.
(30) Allen, W. J.; Bevan, D. R. Steered molecular dynamics simulations reveal important mechanisms in reversible monoamine oxidase B inhibition. *Biochemistry* **2011**, *50*, 6441−6454.
(31) Gentili, F.; Cardinaletti, C.; Vesprini, C.; Ghelfi, F.; Farande, A.; Giannella, M.; Piergentili, A.; Quaglia, W.; Mattioli, L.; Perfumi, M.; Hudson, A.; Pigini, M. Novel ligands rationally designed for characterizing I(2)-imidazoline binding sites nature and functions. *J. Med. Chem.* **2008**, *51* (16), 5130−5134.
(32) Kealey, S.; Turner, E. M.; Husbands, S. M.; Salinas, C. A.; Jakobsen, S.; Tyacke, R. J.; Nutt, D. J.; Parker, C. A.; Gee, A. D. Imaging Imidazoline-I-2 Binding Sites in Porcine Brain Using C-11-BU99008. *J. Nucl. Med.* **2013**, *54* (1), 139−144.